*Journal of the Endocrine Society*, 2024, **8**, 1–8
https://doi.org/10.1210/jendso/bvae049
Advance access publication 12 April 2024
**Research Article**

# 3-[$^{18}$F]Fluoro-*para*-hydroxyphenethylguanidine (3-[$^{18}$F]pHPG) PET—A Novel Imaging Modality for Paraganglioma

**Tobias Else,[1,*] Ka Kit Wong,[2*] Kirk A. Frey,[2] Allen F. Brooks,[2] Benjamin L. Viglianti,[2] and David M. Raffel[2]**

[1]Endocrinology, Metabolism, and Diabetes, University of Michigan, Ann Arbor, MI 48109-5674, USA
[2]Nuclear Medicine/Radiology, University of Michigan, Ann Arbor, MI 48109-0028, USA

**Correspondence:** Ka Kit Wong, MBBS, Department of Nuclear Medicine/Radiology, University of Michigan, 1500 E Medical Center Dr, B1G505 UH, Ann Arbor, MI 48109-0028, USA. Email: kakit@med.umich.edu.
*T.E. and K.K.W. contributed equally to this manuscript as first authors.

## Abstract

**Context:** Functional positron emission tomography (PET) imaging for the characterization of pheochromocytoma and paraganglioma (PCC/PGL) and for detection of metastases in malignant disease, offers valuable clinical insights that can significantly guide patient treatment.

**Objective:** This work aimed to evaluate a novel PET radiotracer, 3-[$^{18}$F]fluoro-*para*-hydroxyphenethylguanidine (3-[$^{18}$F]pHPG), a norepinephrine analogue, for its ability to localize PCC/PGL.

**Methods:** 3-[$^{18}$F]pHPG PET/CT whole-body scans were performed on 16 patients (8 male:8 female; mean age 47.6 ± 17.6 years; range, 19-74 years) with pathologically confirmed or clinically diagnosed PCC/PGL. After intravenous administration of 304 to 475 MBq (8.2-12.8 mCi) of 3-[$^{18}$F]pHPG, whole-body PET scans were performed at 90 minutes in all patients. 3-[$^{18}$F]pHPG PET was interpreted for abnormal findings consistent with primary tumor or metastasis, and biodistribution in normal organs recorded. Standardized uptake value (SUV) measurements were obtained for target lesions and physiological organ distributions.

**Results:** 3-[$^{18}$F]pHPG PET showed high radiotracer uptake and trapping in primary tumors, and metastatic tumor lesions that included bone, lymph nodes, and other solid organ sites. Physiological biodistribution was universally present in salivary glands (parotid, submandibular, sublingual), thyroid, heart, liver, adrenals, kidneys, and bladder. Comparison [$^{68}$Ga]DOTATATE PET/CT was available in 10 patients and in all cases showed concordant distribution. Comparison [$^{123}$I]*meta*-iodobenzylguanidine [$^{123}$I]mIBG planar scintigraphy and SPECT/CT scans were available for 4 patients, with 3-[$^{18}$F]pHPG showing a greater number of metastatic lesions.

**Conclusion:** We found the kinetic profile of 3-[$^{18}$F]pHPG PET affords high activity retention within benign and metastatic PCC/PGL. Therefore, 3-[$^{18}$F]pHPG PET imaging provides a novel modality for functional imaging and staging of malignant paraganglioma with advantages of high lesion affinity, whole-body coregistered computed tomography, and rapid same-day imaging.

**Key Words:** PET/CT, neuroendocrine tumor, pheochromocytoma, paraganglioma

**Abbreviations:** [$^{123}$I]mIBG, [$^{123}$I]*meta*-iodobenzylguanidine; 3-[$^{18}$F]pHPG, 3-[$^{18}$F]fluoro-*para*-hydroxyphenethylguanidine; CT, computed tomography; HNPGL, head and neck paraganglioma; NET, norepinephrine transporter; PCC/PGL, pheochromocytoma and paraganglioma; PRRT, peptide receptor radionuclide therapy; SPECT, single photon emission computed tomography; $SUV_{max}$, maximum standardized uptake value; VMAT, vesicular monoamine transporter.

Pheochromocytoma and paraganglioma (PCC/PGL) are rare tumors arising from the adrenal medulla and paraganglial cells, respectively. PGL can occur anywhere from the skull base to the bladder, typically located in the head and neck area (eg, glomus jugulare, carotid body tumor), in the abdomen (eg, organ of Zuckerkandl), or pelvis (eg, bladder PGL) [1]. Estimates for incidence range between 2 and 8 per million, and for the prevalence between 1:2500 and 1:6500 [2]. Although most textbooks still emphasize the classic presentation with episodic, spell-like hypertension, palpitations, sweating, and pallor, an increasing proportion of patients do not display these symptoms at time of diagnosis [3]. Particularly head and neck paragangliomas (HNPGLs) are most often biochemically silent. Tumors are found incidentally, or less commonly through targeted cross-sectional imaging in symptomatic patients. Although PCC/PGL are usually obvious on magnetic resonance or computed tomography (CT) imaging, the differential diagnosis of these tumors is often broad, ranging from neurogenic tumors (eg, schwannomas) in the head and neck area, to adrenocortical or metastatic tumors in the adrenal gland. Therefore, functional imaging is often used for final confirmatory diagnosis and to determine disease extent and metastatic spread to plan the therapeutic approach [4].

Three functional imaging modalities are currently in widespread use, [$^{123}$I]*meta*-iodobenzylguanidine ([$^{123}$I]mIBG) scintigraphy with single photon emission computed tomography (SPECT)/CT, [$^{18}$F]fluorodeoxyglucose-PET/CT ([$^{18}$F]FDG PET/CT), and [$^{68}$Ga]DOTATATE PET/CT ([$^{68}$Ga]DOTATATE PET/CT) [5, 6]. [$^{123}$I]mIBG scans have a high specificity, but low sensitivity, particularly for metastatic disease and nonfunctional PCC/PGL. In addition, imaging is an inconvenient, multiday procedure, also requiring iodine

**Received:** 11 December 2023. **Editorial Decision:** 7 March 2024. **Corrected and Typeset:** 12 April 2024

pretreatment for thyroid protection. [$^{18}$F]FDG PET/CT and [$^{68}$Ga]DOTATATE PET/CT are highly sensitive, but often lack specificity. Particularly inflammatory changes, such as benign reactive lymph nodes and, in the case of [$^{68}$Ga]DOTATATE PET/CT, other tumors, such as neuroendocrine tumors, thyroid cancers, and meningiomas occur as false-positive findings. None of these functional scans provides excellent sensitivity and specificity in the same imaging modality, making it difficult to standardize imaging algorithms.

We had previously reported 3-[$^{18}$F]pHPG, a compound chemically related to [$^{123}$I]mIBG, for cardiac sympathetic nerve imaging in normal individuals [7] and in heart failure patients [8], and feasibility for imaging metastatic PGL, based on its characteristics as a substrate for catecholamine transporters [9]. Here we show that 3-[$^{18}$F]pHPG can be used as a highly specific and sensitive functional imaging tracer for functional and nonfunctional PCC/PGL. In addition, we report the biodistribution of 3-[$^{18}$F]pHPG in tumor tissues and normal organs (liver, heart, kidneys) and compare its performance to that of [$^{68}$Ga]DOTATATE PET/CT.

## Materials and Methods

### Patients

The study protocol was approved by the Medical School Institutional Review Board and written informed consent was obtained from all participants. 3-[$^{18}$F]pHPG in PCC/PGL was performed under an exploratory investigational new drug clearance from the US Food and Drug Administration. Patients with suspected PCC or PGL, including those with planned surgical resection and those with biopsy-proven or clinically diagnosed metastatic disease, were eligible. Participants were nonconsecutive, based on exploratory indications for imaging of PCC/PGL, and recruited by multiple methods, through endocrinology and endocrine oncology clinics and medical record searches of functional imaging scans relevant to PGL/PCC and informational flyers.

[$^{68}$Ga]DOTATATE PET/CT scans were clinically available for 10 patients (7 of these were within the preceding year before study recruitment); however, 1 patient had peptide receptor radionuclide therapy (PRRT) between the [$^{68}$Ga]DOTATATE PET/CT; therefore, it could not be directly compared. One patient (No. 2) had surgical intervention between the PET scans that had to be accounted for. Current [$^{123}$I]mIBG scan comparison was present in 2 patients and another 2 patients had a [$^{123}$I]mIBG scan obtained as part of the research study to demonstrate noninferiority of 3-[$^{18}$F]pHPG PET. One patient had a [$^{123}$I]mIBG scan that was greater than 10 years old and not usable. Patients were prepared according to current guidelines recommending that antihypertensive medications that could potentially interfere with the uptake mechanism be stopped prior to PET imaging [10]. Five patients were on doxazosin at the time of imaging and one patient was on metoprolol and amlodipine, and these medications were not discontinued.

### 3-[$^{18}$F]Fluoro-*para*-hydroxyphenethylguanidine Synthesis

For the first 6 participants, 3-[$^{18}$F]pHPG was prepared using an iodonium salt precursor, as previously reported [11]. After this, a new radiosynthetic method employing a spirocyclic iodonium ylide precursor, based on a previous approach developed for its structural isomer 4-[$^{18}$F]mHPG (Fig. 1), which provides higher radiochemical yields, was used [12].

### 3-[$^{18}$F]Fluoro-*para*-hydroxyphenethylguanidine Positron Emission Tomography Imaging

Whole-body PET/CT scans were acquired on a Siemens Biograph TruePoint True V PET/CT camera following intravenous injection of between 304 and 475 MBq (8.2-12.8 mCi) of 3-[$^{18}$F]pHPG, at 90 minutes (N = 16) and 180 minutes (N = 10) post injection. Data were reconstructed with 3D-OSEM software using the following parameters: time-of-flight enabled, 3 iterations 21 subsets, resolution modeling, and a 5-mm Gaussian post filter. The PET matrix size was $200 \times 200$ with a pixel size $2.67 \times 2.67$ mm$^2$ and slice thickness of 3 mm. The noncontrast, free-breathing CT was performed in low-dose mode (120 kVp; 80 mAs, CAREDOSE dose reduction enabled).

### Adverse Events and Safety Monitoring

Safety monitoring for adverse events consisted of physical examination before PET, vital signs, electrocardiogram before and after radiotracer injection, laboratory testing parameters (blood samples for complete blood count, comprehensive metabolic panel, plasma metanephrines/normetanephrines and plasma catecholamines (norepinephrine, epinephrine, dopamine), and urine sample for urinalysis. Follow-up calls to the patient to screen for adverse effects were made by the study coordinator 24 hours and 30 days after PET scanning. For all female participants of childbearing potential (aged 18 years to menopause), a negative urine pregnancy test was confirmed before PET scanning.

### 3-[$^{18}$F]Fluoro-*para*-hydroxyphenethylguanidine Positron Emission Tomography Imaging Interpretation

3-[$^{18}$F]pHPG 90-minute images were reviewed using the viewer software with fusion capability, MIM software package (MIM Software) for pathological radioactivity foci in the adrenals, soft tissues of the abdomen, thorax, pelvis, and neck, and physiological biological distributions and normal variants were noted. For the first 10 patients, the 90-minute images were viewed side by side with the 180-minute images and comparison between time points for differences in lesion detection rate and conspicuity were made. Analyses were performed to compare retention of 3-[$^{18}$F]pHPG in target organs, liver, thyroid, adrenals, and lumbar spine using semiquantitative uptake parameters (standardized uptake value; $SUV_{mean}$, $SUV_{max}$), and changes over time were recorded. Images were interpreted by a single reader (K.K.W.) with access to clinical context and indications for the PET scan, initially blinded to laboratory, functional, and anatomical imaging, then subsequently unblinded.

## Results

### 3-[$^{18}$F]Fluoro-*para*-hydroxyphenethylguanidine Synthesis

The iodonium salt precursor method of 3-[$^{18}$F]pHPG preparation (N = 6) yielded activities averaging $0.70 \pm 0.25$ GBq (range, 0.44-1.08 GBq), radiochemical purities averaged $98.6\% \pm 0.9\%$ (range, 98.0-99.8%), molar activities averaged $123 \pm 81$ GBq/μmol (range, 44-224 GBq/μmol), and injected masses averaged $1.12 \pm 1.00$ μg (range, 0.39-2.79 μg). For the iodonium ylide precursor method (N = 10), radiochemical yields averaged $4.0 \pm 1.3$ GBq (range, 1.8-6.9 GBq), radiochemical

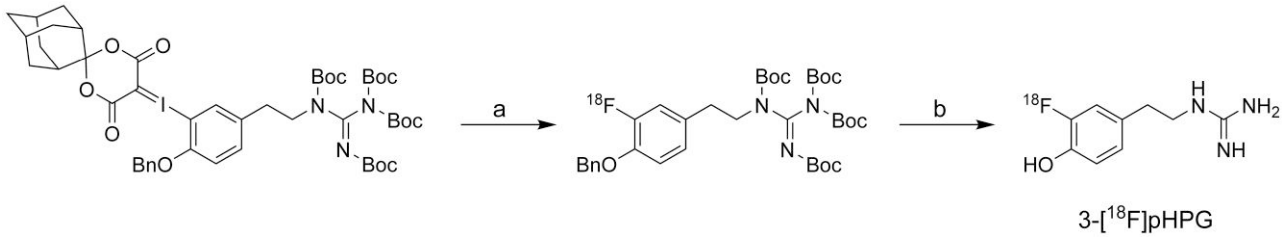


**Figure 1.** Radiosynthesis of 3-[$^{18}$F]fluoro-*para*-hydroxyphenethylguanidine (3-[$^{18}$F]pHPG). a, A spirocyclic iodonium ylide precursor with protecting groups on the amine and hydroxyl groups is reacted with $^{18}$F-fluoride ion at 120°C for 10 minutes. b, After cooling, 3.0 N HBr is added and the solution heated at 120°C for 15 minutes to remove the protecting groups. 3-[$^{18}$F]pHPG is purified using high-performance liquid chromatography as a sterile injectable solution.

purities averaged 99.2% ± 0.2% (range, 99.4%-100%), molar activities averaged 153 ± 93 GBq/μmol (range, 81-406 GBq/μmol), and injected masses averaged 0.78 ± 0.27 μg (range, 0.27-1.19 μg).

## Patient Clinical Data (Demographics, Genetics, and Prior Therapies)

Sixteen patients (8 male:8 female, mean age 47.6 ± 17.6 years, range, 19-74 years) with a confirmed or suspected diagnosis of PCC/PGL were included in this study (Table 1). Primary tumors (nodules) were in the adrenal gland (N = 8), retroperitoneum (N = 4), and head and neck region (N = 4). Nine patients had a genetic predisposition syndrome (*SDHB* = 5, *SDHD* = 2, *VHL* = 2). Nine patients were imaged at initial presentation and the remaining 7 patients were imaged later in the course with documented metastatic disease, one of whom had prior resection of lung metastases. One patient had an additional pancreatic neuroendocrine tumor, another had a prior ileal neuroendocrine tumor resected, and one had an undetermined positive lesion in the calvarium on [$^{68}$Ga]DOTATATE PET/CT. Prior treatments for metastatic disease included monthly somatostatin analogue treatment, external beam radiation treatment, [$^{90}$Y]-embolization of the liver, [$^{177}$Lu]DOTATATE therapy, [$^{131}$I]mIBG therapy, and capecitabine/temozolomide (Table 2).

## Safety Monitoring and Adverse Event Reporting

Safety data did not show any grade 3 to 4 adverse reactions. None of the participants reported any clinical symptoms of chest pain, hypertension, or tachycardia during the study acquisition and follow-up period. There were no significant changes between baseline and following PET for the electrocardiogram, complete blood count, laboratory panels of norepinephrine/epinephrine or metanephrine panels in any of our patients after completion of PET imaging. Some individuals reported symptoms that were mild and not considered related to an effect of the 3-[$^{18}$F]pHPG administration. Reported symptoms included lower back pain following the PET scan, fatigue following the PET scan, fatigue and headache attributed to migraine, and shakiness and light-headedness the day of the scan that may have been due to dehydration prior to the imaging. One participant (No. 1) had albumin of 2.5 g/dL considered a G2 hypoalbuminemia. One participant (No. 5) had an elevated white cell count before and after the PET scan.

## Physiologic Distribution of Radiotracer

Physiological uptake of 3-[$^{18}$F]pHPG was universally found in the salivary glands (parotids [$SUV_{max}$ left 6.7 ± 2.1 SD, $SUV_{max}$ right 7.3 ± 3.1 SD], submandibular and sublingual) and thyroid ($SUV_{max}$ 6.1 ± 3.0 SD), likely related to sympathetic innervation of these organs. 3-[$^{18}$F]pHPG tracer uptake was also observed in the myocardium ($SUV_{max}$ left ventricle 11.2 ± 3.3 SD) despite the fact that several patients had significantly elevated metanephrine or normetanephrine levels. The liver showed some heterogeneity with a gradient of having more intense activity in the left lobe compared to the right lobe. Renal excretion of radiotracer and accumulation in the bladder was also noted. Normal adrenal glands showed intense 3-[$^{18}$F]pHPG uptake including in patients with prior unilateral adrenalectomy ($SUV_{max}$ left 11.4 ± 4.9 SD, $SUV_{max}$ right 9.1 ± 2.0 SD). These findings are similar to the known distributions of [$^{123}$I]mIBG. Interestingly, in half of the patients there was a diffuse moderate activity distribution of 3-[$^{18}$F]pHPG in the pancreas, not usually described on [$^{123}$I]mIBG scans (Table 3).

Endometrial uptake of 3-[$^{18}$F]pHPG was observed in some though not all female participants (N = 6). A study of uterine sympathetic innervation using the sympathetic nerve markers tyrosine hydroxylase and neuropeptide Y reported the autonomic sympathetic marker tyrosine hydroxylase was present in all layers of mature fetal uterine tissue, especially in the cervix, and neuropeptide Y was present in all layers, especially the myometrium and endometrium [13], suggesting sympathetic innervation of the uterus to underline this observed distribution. Prostate gland uptake was present in one patient. One patient had linear uptake in the esophagus, possibly due to inflammatory changes (eosinophilic esophagitis). One patient had uptake of 3-[$^{18}$F]pHPG in brown adipose tissue in the neck. In one patient a focus of dural uptake on [$^{68}$Ga]DOTATATE PET/CT was not visualized in the 3-[$^{18}$F]pHPG scan, suggesting a benign meningioma as an underlying diagnosis. One patient had a concurrent pancreatic neuroendocrine tumor, which did not show 3-[$^{18}$F]pHPG uptake. In one patient a small, mild, indeterminate thoracic paraspinal focus was observed that did not show any correlate on cross-sectional imaging. This patient has a benign pheochromocytoma and did not have any other metastatic disease, suggesting that this uptake was due to either brown fat or a small paraganglion.

## Positron Emission Tomography Findings of Pathological Primary and Secondary Lesions

3-[$^{18}$F]pHPG PET was used to evaluate PCC in 5 patients. Two patients presented with large adrenal masses and elevated catecholamine levels, and their adrenal masses had intense 3-[$^{18}$F]pHPG uptake confirming PCC, without any metastatic sites

**Table 1. Patient demographics and diagnosis**

| Pt No. | Sex | Age, y | Diagnosis | Genetic predisposition | Malignant behavior | Other tumors |
|---|---|---|---|---|---|---|
| 1 | Male | 30 | Abdominal paraganglioma | *SDHB* germline PV | Metastatic to bones and lymph nodes | None |
| 2 | Female | 43 | Abdominal paraganglioma | Sporadic loss of IHC for *SDHB*, *NF1* variant mosaicism | Metastatic to bones, lymph nodes, and liver | None |
| 3 | Male | 59 | Left-sided pheochromocytoma | Sporadic | Metastatic to abdominal and thoracic lymph nodes | None |
| 4 | Male | 24 | Abdominal paraganglioma | *SDHB* germline PV | Oligometastatic to bones | None |
| 5 | Female | 19 | Right-sided pheochromocytomas (2) | *VHL* germline PV | None to date | Pancreatic neuroendocrine tumor |
| 6 | Female | 45 | Left-sided pheochromocytoma | sporadic | Oligometastatic to lungs | None |
| 7 | Female | 53 | Abdominal paraganglioma | Sporadic | None to date | None |
| 8 | Male | 61 | Right-sided pheochromocytoma | Sporadic | None to date | None |
| 9 | Male | 72 | Abdominal paraganglioma invasive to left kidney | Sporadic | Metastatic to liver, bone, abdominal, and thoracic lymph nodes | None |
| 10 | Female | 25 | Head and neck paraganglioma | *SDHD* germline PV | None to date | None |
| 11 | Female | 50 | Head and neck paraganglioma | *SDHB* germline PV | None to date | Ileal neuroendocrine tumor not present on 3-[$^{18}$F] pHPG PET |
| 12 | Female | 49 | Head and neck paraganglioma | *SDHB* germline PV | None to date | None |
| 13 | Male | 69 | Malignant pheochromocytoma | Sporadic | Metastatic to thoracic and supraclavicular lymph nodes | None |
| 14 | Female | 74 | Head and neck paraganglioma | *SDHD* germline PV | None to date | Prior glomus tympanicum and glomus jugulare tumors |
| 15 | Male | 56 | Right-sided pheochromocytoma | Sporadic | None to date | None |
| 16 | Male | 31 | Left-sided adrenal nodule | *VHL* germline PV | None to date | Renal cell cancer |

Abbreviations: IHC, immunohistochemistry; NF1 neurofibromatosis Type 1; PET, positron emission tomography; 3-[$^{18}$F]pHPG; 3-[$^{18}$F]fluoro-*para*-hydroxyphenethylguanidine; Pt, patient; PV, pathogenic variant; SDHB, succinate dehydrogenase subunit B gene; SDHD, succinate dehydrogenase subunit D gene; VHL, von Hippel-Lindau gene.

**Table 2. Treatments**

| Pt No. | Surgery | BP meds | Metanephrine, plasma, nmol/L | Normetanephrine, plasma, nmol/L | Treatments |
|---|---|---|---|---|---|
| 1 | Right partial adrenalectomy | Doxazosin | <0.2 | 4.2 | Zoledronic acid, octreotide LAR every 4 wk |
| 2 | Retroperitoneal paraganglioma resection | — | <0.2 | 4.6 | None to date |
| 3 | Left adrenalectomy | — | 0.7 | 31 | [$^{131}$I]-mIBG |
| 4 | Thoracic spine fusion surgery | — | <0.2 | 0.4 | EBRT to T6 spine |
| 5 | Left adrenalectomy | — | <0.2 | 0.8 | None to date |
| 6 | Right adrenalectomy, lung nodule resection | — | <0.2 | 0.6 | None to date |
| 7 | Perihepatic paraganglioma resection | Doxazosin | <0.2 | 3 | None to date |
| 8 | Right adrenalectomy | Doxazosin | <0.2 | 7.8 | None to date |
| 9 | Pararenal paraganglioma resection and radical left nephrectomy | Doxazosin | 1.9 | 3.1 | capecitabine/temozolomide, octreotide LAR every 4 wk, liver [$^{90}$Y]-Theraspheres (×2), EBRT to spine |
| 10 | None to date | — | 7.5 | 4.2 | None to date |
| 11 | None to date | — | <0.2 | 24.5 | Observation |
| 12 | None to date | — | 0.2 | 0.5 | Observation |
| 13 | Right adrenalectomy | — | 0.2 | 1.6 | EBRT to T12, capecitabine and temozolomide, PRRT |
| 14 | Head and neck paraganglioma resection | Metoprolol, amlodipine | 0.2 | 5.8 | None to date |
| 15 | Right adrenalectomy | Doxazosin | <0.2 | 0.5 | None to date |
| 16 | None to date | — | 0.2 | 2.2 | None to date |

Abbreviations: BP, blood pressure; EBRT, external beam radiation therapy; LAR, long-acting release; PRRT, peptide receptor radionuclide therapy; Pt, patient.

**Table 3. Standardized uptake values in organs and disease sites**

| No. | Lt parotid ($SUV_{max}$) | Rt parotid ($SUV_{max}$) | Thyroid ($SUV_{max}$) | Left ventricle ($SUV_{max}$) | Aortic arch ($SUV_{mean}$) | Liver ($SUV_{mean}$) | Lt adrenal ($SUV_{max}$) | Rt adrenal ($SUV_{max}$) | Soft tissue lesion ($SUV_{max}$) | Bone lesion ($SUV_{max}$) | Soft tissue location |
|---|---|---|---|---|---|---|---|---|---|---|---|
| 1 | 3.3 | 3.3 | 10.0 | 16.7 | 0.8 | 4.2 | 21.2 | RAR | 74.8 | 145.0 | Right adrenal bed |
| 2 | 6.3 | 6.1 | 5.4 | 13.5 | 0.5 | 0.9 | 12.4 | 7.9 | 4.1 | 38.7 | Retroperitoneal surgical bed |
| 3 | 5.2 | 4.9 | 1.8 | 6.3 | 0.7 | 4.4 | LAR | 1.3 | 5.3 | None | Left pararenal lymph nodes |
| 4 | 5.2 | 6.5 | 7.3 | 9.3 | 0.6 | 2.7 | 7.3 | 11.2 | None | 48.7 | None |
| 5 | 6.4 | 7.8 | 12.0 | 15.7 | 0.3 | 3.0 | LAR | 12.1 | 12.1. | 3.2 | Difficult to define tumor separate from right adrenal due to small size, mild focus at level of T7 spine with SUVmax = 3.2 |
| 6 | 3.3 | 2.9 | 5.0 | 12.1 | 0.4 | 3.5 | 11.8 | RAR | None | None | Dural lesion seen on DOTATATE PET, likely meningioma with no 3-[$^{18}$F]pHPG uptake |
| 7 | 8.0 | 10.9 | 5.0 | 9.5 | 0.4 | 2.9 | 7.7 | 6.6 | 7.1 | None | 3.6-cm cystic mass between liver, IVC, and diaphragmatic crus |
| 8 | 5.8 | 4.0 | 5.1 | 11.1 | 0.6 | 2.4 | 11.7 | pheo | 24.1 | None | Right adrenal mass measuring 3.1 × 2.6 cm |
| 9 | 6.0 | 4.9 | 5.3 | 9.4 | 0.7 | 2.8 | 11.0 | RAR | 103.0 | 73.0 | Numerous liver lesions |
| 10 | 10.0 | 8.9 | 5.7 | 11.0 | 0.8 | 2.4 | 8.7 | 10.0 | 2.2 | None | Left jugular foramen mass |
| 11 | 7.5 | 9.9 | 1.8 | 8.7 | 0.6 | 3.1 | 9.4 | 8.1 | 20.2 | None | Left jugular foramen mass |
| 12 | 11.0 | 14.0 | 7.8 | 13.0 | 0.8 | 3.1 | 9.9 | 7.2 | 2.2 | None | Right carotid body mass |
| 13 | 8.4 | 7.8 | 10.9 | 17.0 | 1.0 | 5.3 | 20.5 | RAR | 23.4 | None | Left supraclavicular lymph node |
| 14 | 7.6 | 10.9 | 7.9 | 11.5 | 0.6 | 4.4 | 16.7 | 11.1 | 6.6 | None | Left carotid body mass |
| 15 | 6.9 | 7.6 | 2.8 | 6.5 | 1.1 | 3.1 | 4.5 | pheo | 16.1 | None | Right adrenal mass measuring 7.5 cm |
| 16 | 6.5 | 7.0 | 4.3 | 8.3 | 0.5 | 2.7 | 7.9 | 7.5 | 4.6 | None | Left adrenal nodule measuring 0.9 cm with SUVmax 4.6 < than adjacent normal adrenal |

Abbreviations: IVC, inferior vena cava; LAR, left adrenal resection; Lt., left; pheo, pheochromocytoma; PET, positron emission tomography; 3-[$^{18}$F]pHPG, 3-[$^{18}$F]fluoro-*para*-hydroxyphenethylguanidine; RAR, right adrenal resection; Rt., right; $SUV_{max}$, maximum standardized uptake value.

(Fig. 2). These 2 patients had concurrent [$^{68}$Ga]DOTATATE PET/CT that were positive and 1 also had [$^{18}$F]FDG PET/CT; all 3 PET scans were positive in this individual (patient 15). In 2 patients with VHL and 1 with SDHB predisposition, with small adrenal nodules suspected to be PCC, 3-[$^{18}$F]pHPG activity was difficult to attribute to the tumor as opposed to normal adrenal tissue, which had high 3-[$^{18}$F]pHPG uptake. One patient with small PCC required coregistration to magnetic resonance imaging to be confident of uptake; however, with intense uptake in normal adrenals it may be difficult to distinguish small (<1 cm) PCC even on PET imaging.

3-[$^{18}$F]pHPG PET was used to evaluate 1 patient with abdominal PGL and 4 patients with suspected HNPGL. The patient with abdominal PGL had mild uptake with $SUV_{max}$ of 7.1 in the cystic mass between the liver and diaphragmatic crus, somewhat obscured by adjacent liver activity. Two HNPGLs had intense uptake confirming their PGL diagnosis; a third had mild though positive uptake, also confirmatory of HNPGL. The remaining patient with HNPGL had minimal activity, and the scan was considered negative despite genetic predisposition syndrome.

Regarding sites of metastatic disease in 6 patients, 3-[$^{18}$F]pHPG localizes intensely within metastases to bone, lymph nodes, local soft tissue recurrences, and solid organ metastases (liver and lungs) (Fig. 3). 3-[$^{18}$F]pHPG PET was able to detect recurrent soft tissue disease in the retroperitoneal surgical bed (patient 2), in the adrenal surgical bed (patient 1), and within the abdominal and supraclavicular lymph nodes (patients 3, 8, and 13). Intense focal 3-[$^{18}$F]pHPG uptake in multifocal osseous lytic lesions was found in 4 patients. [$^{68}$Ga]DOTATATE PET scans were available for 5 of these 6 patients with overall similar lesion detection rates for sites of osseous metastatic disease. Notably, in one patient there was a better visualization of liver metastasis with 3-[$^{18}$F]pHPG PET than with [$^{68}$Ga]DOTATATE PET, attributed to lower background hepatic 3-[$^{18}$F]pHPG uptake. Two patients with osseous metastases had a [$^{123}$I]mIBG scan performed as part of the study design, and 3-[$^{18}$F]pHPG PET demonstrated more metastatic lesions with higher target to background than the planar [$^{123}$I]mIBG images (Fig. 4). The remaining 2 participants with a recent clinical [$^{123}$I]mIBG scan had concurrent findings of abdominal PGL and oligometastatic bone disease, respectively.

The first 10 patients had 2 time points for 3-[$^{18}$F]pHPG PET at 90 minutes and 180 minutes. Visual comparison between these time points viewed side by side found no differences in lesion detection rate and conspicuity; therefore, the later

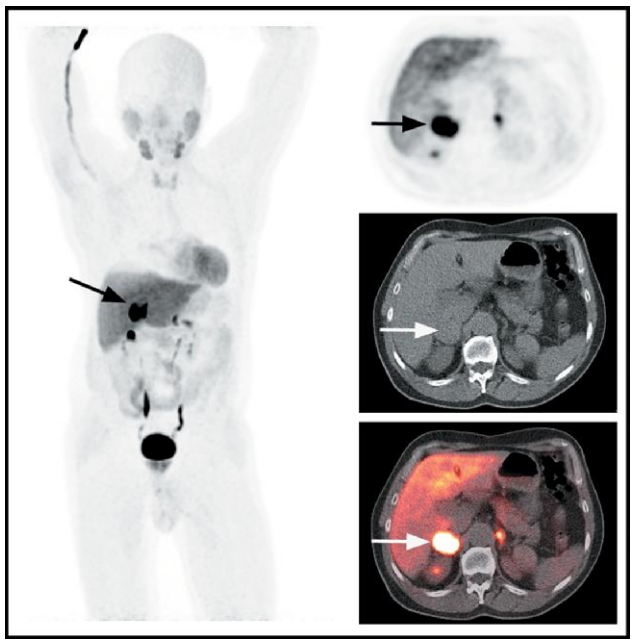

**Figure 2.** A 61-year-old man (patient 8) presented with a right adrenal mass and elevated metanephrine levels. Positron emission tomography (PET) imaging at 90 minutes following intravenous injection of 445 MBq (12.3 mCi) of 3-[$^{18}$F]fluoro-*para*-hydroxyphenethylguanidine (3-[$^{18}$F] pHPG). Left: Maximum intensity projection (MIP) imaging of the 3-[$^{18}$F] pHPG scan shows uptake in a right adrenal mass (arrow) with a standardized uptake value ($SUV_{max}$) of 24.1. 3-[$^{18}$F]pHPG activity is also seen in the parotid glands, thyroid, heart, liver, and left adrenal, with genitourinary excretion of radiotracer in the kidneys and bladder. Right: Axial slices PET (top), computed tomography (CT) (middle), and PET/CT (bottom) show intense 3-[$^{18}$F]pHPG activity in the right pheochromocytoma (arrows).

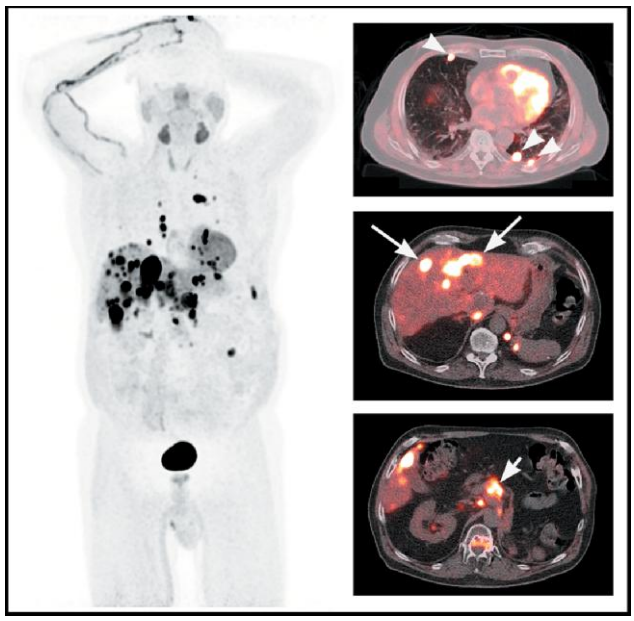

**Figure 3.** A 72-year-old man (patient 9) with a metastatic neuroendocrine tumor underwent radical left nephrectomy and had resection of a left pararenal mass. Postoperatively he had high normetanephrines, and urinary norepinephrine and dopamine levels. Positron emission tomography (PET) imaging was performed following intravenous injection of 306 MBq (8.3 mCi) of 3-[$^{18}$F] fluoro-*para*-hydroxyphenethylguanidine (3-[$^{18}$F]pHPG). Left: 3-[$^{18}$F]pHPG MIP image at 90 minutes demonstrates multifocal metastases in the liver (standardized uptake value [$SUV_{max}$] of 103), abdominal and thoracic lymph nodes, lungs, and bones ($SUV_{max}$ of 73). 3-[$^{18}$F]pHPG activity is also seen in the parotid glands, thyroid, heart, liver, and pancreas, and there is genitourinary excretion of radiotracer in the kidneys and bladder. Right: Axial fused PET/CT slices showing intense 3-[$^{18}$F]pHPG activity in malignant disease in the lungs (arrowheads, top), liver (long arrows, middle), and retroperitoneal abdominal nodes (short arrow, bottom). There is uptake in lytic/sclerotic bone metastases in the thoracic spine (bottom).

time point of 180 minutes was removed from the protocol for subsequent patients.

## Discussion

Our findings demonstrate favorable kinetic properties of 3-[$^{18}$F]pHPG PET imaging of PCC/PGL. This is a norepinephrine analogue that shows uptake in neurosecretory vesicles of peripheral sympathetic nerves via the norepinephrine transporter (NET) and the second isoform of the vesicular monoamine transporter (VMAT2). We have previously reported a case demonstrating the potential of 3-[$^{18}$F]pHPG PET for staging of metastatic PGL [9]. The present study confirms the excellent spatial resolution of 3-[$^{18}$F]pHPG PET in depicting metastatic PCC/PGL at various bone and soft tissue locations, and also extends the utility of 3-[$^{18}$F]pHPG PET imaging of PCC/PGL in a range of indications: for preoperative characterization of adrenal nodules in primary PCC and exclusion of concurrent PGL or metastases prior to surgery, characterization of a subset of HNPGL, and use in different genetic predisposition syndromes. Although we have only 4 comparisons to date, in 2 patients with widespread multifocal bone metastases 3-[$^{18}$F]pHPG PET imaging appeared superior to planar [$^{123}$I]mIBG scintigraphy. Advantages that are readily apparent are same-day functional imaging, higher spatial resolution of PET technology, whole-image hybrid PET/CT correlation, and lower overall radiation exposure. Additionally, 90-minute uptake appears adequate with no increased lesion detection rate compared to 180 minutes, which is convenient for patient throughput and comparable to protocols with [$^{18}$F]FDG PET/CT. Also for 3-[$^{18}$F]pHPG PET, there is no need for thyroid radioprotection with supersaturated potassium iodide drops or Lugol's iodine, as is the case for [$^{123}$I] mIBG when the pharmacy source of [$^{123}$I] iodine may have longer-lived radioiodine isotopes requiring thyroid blocking of dissociated radioiodine isotopes. The administration of 3-[$^{18}$F]pHPG was safe and did not result in any pharmacological effects, and no serious clinical adverse events were observed. Although the same medications described affecting [$^{123}$I]mIBG tumor uptake could theoretically alter uptake for 3-[$^{18}$F]pHPG, the imaging quality was excellent in patients that remained on doxazosin for blood pressure control.

3-[$^{18}$F]pHPG PET detected primary adrenal tumors and abdominal PGL. The uptake and retention of 3-[$^{18}$F]pHPG PET is characteristic of PCC and PGL, confirming the clinical and imaging diagnosis. It also affords whole-body screening and indicates the solitary nature of the lesion prior to surgery, indicating benign tumors. HNPGLs are often nonfunctioning and may not be well visualized with [$^{123}$I]mIBG, therefore [$^{111}$In]-DTPA-pentetreotide, [$^{68}$Ga]DOTATATE PET, and [$^{18}$F]DOPA PET have been proposed and reported to have superior sensitivity to [$^{123}$I]mIBG. Nonetheless, 3 of 4 HNPGL patients in the present study showed uptake of 3-[$^{18}$F] pHPG, albeit with a wide range of intensity, confirmatory of

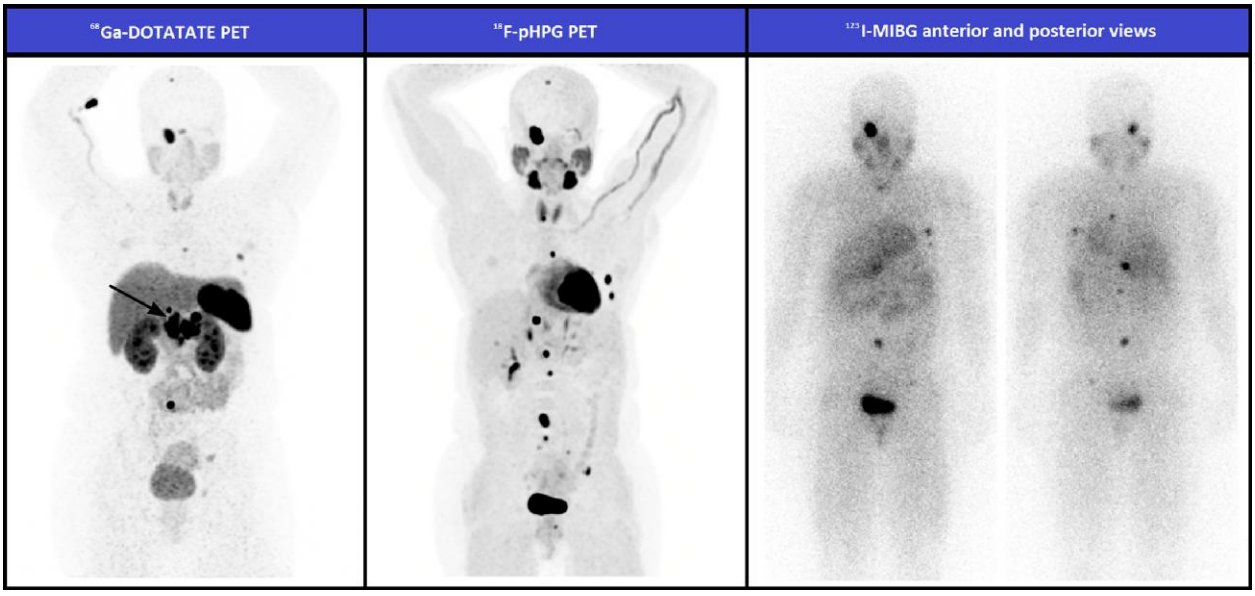


**Figure 4.** A 43-year-old woman (patient 2) with metastatic paraganglioma. Comparison between left: [$^{68}$Ga]DOTATATE PET, middle: 3-[$^{18}$F]pHPG PET, and right: [$^{123}$I]mIBG scan. She initially presented with preeclampsia and was found to have a large abdominal paraganglioma. Clinically she had worsening hypertension, palpitations, lightheadedness, and shortness of breath. Computed tomography scan revealed a mass posterior to the pancreas, between the aorta and vena cava, and there was metastatic osseous disease in the right orbital ridge and in the thoracic and lumbar spine (standardized uptake value [$SUV_{max}$] of 38.7). She underwent exploratory celiotomy and excision of retropancreatic paraganglioma (arrow), seen on the preoperative [$^{68}$Ga]DOTATATE PET, which has been surgically resectioned on the postoperative 3-[$^{18}$F]pHPG PET. 3-[$^{18}$F]pHPG PET and [$^{68}$Ga]DOTATATE PET had similar detection of osseous metastases, though 3-[$^{18}$F]pHPG PET detected a liver metastases ($SUV_{max}$ of 4.1) not evident on [$^{68}$Ga]DOTATATE PET, likely due to lower background hepatic activity. 3-[$^{18}$F]pHPG PET detected more bone metastases than the comparison postoperative [$^{123}$I]mIBG scan.

PGL, with the remaining patient having low uptake that was considered negative (without pathological diagnosis presently). A concurrent pancreatic neuroendocrine tumor in one patient did not show any uptake, suggesting a higher specificity of 3-[$^{18}$F]pHPG compared to [$^{68}$Ga]DOTATATE PET for PCC/PGL, potentially useful for the differential diagnosis of PCC/PGL vs other neuroendocrine tumors. Background physiologic uptake was present in several organs, including the adrenal gland and pancreas. While the adrenal gland uptake might hamper the evaluation of small PCC, there is little clinical relevance to these tumors. All patients with small presumed PCC in this study were currently under clinical observation and entirely asymptomatic. Regarding thoracic PGL, since there is intense myocardial uptake that is related to the cardiac sympathetic innervation, the CT component of the PET/CT acquisition is helpful to distinguish a 3-[$^{18}$F]pHPG-avid paracardial mass as distinct from the heart.

The use of 3-[$^{18}$F]pHPG for staging and restaging of metastatic disease was excellent and detected bone, liver, lung, and nodal metastatic disease and soft tissue local recurrences in 6 patients. In another patient the scan was equivocal, though likely an incidental benign paraspinous ganglion or atypical uptake in brown fat. 3-[$^{18}$F]pHPG was able to detect recurrent soft tissue disease in retroperitoneal and adrenal surgical beds and within abdominal lymph nodes and supraclavicular nodes. There was intense focal 3-[$^{18}$F]pHPG uptake in multifocal osseous lytic lesions. In one patient there was a liver-predominant pattern of metastatic disease.

Interestingly, benign diffuse pancreas activity was present in 8 patients, similar to what has been reported about [$^{18}$F]-*meta*-fluorobenzylguanidine, a different mIBG analogue [14, 15]. This may be related to VMAT2-related uptake in the pancreas. One of the unique properties of 3-[$^{18}$F]pHPG that is interesting is that it is effectively trapped in norepinephrine storage vesicles, which potentially may be an advantage of this tracer over other agents being developed for imaging these tumors [8].

Parallel [$^{68}$Ga]DOTATATE PET scans were available for patients with metastatic disease with overall similar lesion detection rate for sites of soft tissue and osseous metastatic disease. [$^{68}$Ga]DOTATATE PET has high sensitivity for PCC/PGL [16, 17] and a potential advantage for HNPGL [18]. Notably in one patient there was slightly better conspicuity of liver foci on the 3-[$^{18}$F]pHPG PET vs [$^{68}$Ga]DOTATATE PET, possibly due to less background hepatic radiotracer concentration. In 2 patients in whom a research [$^{123}$I]mIBG study was ordered, the lesion detection was clearly superior on 3-[$^{18}$F]pHPG PET. Thus, despite excellent performance of [$^{68}$Ga]DOTATATE PET with somatostatin receptor expression, 3-[$^{18}$F]pHPG could be more specific for metastatic disease, or can offer complementary performance, particularly considering the negative 3-[$^{18}$F]pHPG PET findings in our participants with pancreatic neuroendocrine tumor and meningioma. However, we certainly have seen potential false positives related to brown fat and endometrium. We envision that 3-[$^{18}$F]pHPG PET could replace [$^{123}$I]mIBG scintigraphy (providing it remains a surrogate to establish eligibility for [$^{131}$I]mIBG therapy) and used as a first functional imaging modality for PCC/PGL characterization and staging, reserving [$^{68}$Ga]DOTATATE PET for patients with pathology-proven PCC/PGL, known to have low NET and VMAT1/2 expression.

Limitations of this study are the small numbers of patients having 3-[$^{18}$F]pHPG PET for different indications, although we intend to perform patient-level and lesion-level statistical analyses for diagnostic efficacy of 3-[$^{18}$F]pHPG PET and

comparison with other imaging, at completion of recruitment. Future studies will need to evaluate tumor characteristics for PCC/PGL associated with the different genetic syndromes. Additional neoplasms including carcinoids, medullary thyroid cancer, and neuroblastoma also express NET and VMAT1/2; however, exploration of these disease was outside the scope of funding for the present study and we did not recruit any with the exception of the patient with concurrent pancreatic neuroendocrine tumor. Finally, it is it is not known whether 3-[$^{18}$F]pHPG PET could be used to select patients for [$^{131}$I]mIBG therapy. However, an important avenue for future investigation is the development of a β-emitter or α-emitter analogue of 3-[$^{18}$F]pHPG itself that could be combined with 3-[$^{18}$F]pHPG PET to provide a treatment option for patients with malignant PCC/PGL.

### Conclusion

We found high activity of 3-[$^{18}$F]pHPG PET in PCC/PGL, both in primary PCC and PGL, as well as metastatic disease. 3-[$^{18}$F]pHPG PET has the potential for convenient, single-day, high-resolution PET/CT imaging of PCC and PGL for primary lesion characterization, staging, and metastatic survey. In this pilot study, 3-[$^{18}$F]pHPG PET was superior to [$^{123}$I]mIBG scintigraphy in the presence of widespread metastatic disease and comparable to [$^{68}$Ga]DOTATATE PET. Future considerations are development of an analogue of 3-[$^{18}$F]pHPG radiolabeled with a particle-emitting radionuclide as a companion therapeutic agent for treatment of metastatic disease.

## Acknowledgments

The authors wish to thank James Pool Jr for his time and assistance with running this study.

## Funding

This work was supported by a Neuroendocrine Tumor Research Foundation (NETRF) Investigator Award (No. 657755).

## Disclosures

K.K.W., D.R., B.L.V., A.F.B., and K.A.F. have nothing to declare. T.E. has received honoraria from participation in scientific advisory boards for Lantheus, HRA Pharma, and Merck.

## Data Availability

Some or all data sets generated during and/or analyzed during the current study are not publicly available but are available from the corresponding author on reasonable request.

## References

1. Lenders JW, Duh QY, Eisenhofer G, *et al*. Pheochromocytoma and paraganglioma: an endocrine society clinical practice guideline. *J Clin Endocrinol Metab*. 2014;99(6):1915-1942.
2. Kiernan CM, Solórzano CC. Pheochromocytoma and paraganglioma: diagnosis, genetics, and treatment. *Surg Oncol Clin N Am*. 2016;25(1):119-138.
3. Ebbehoj A, Stochholm K, Jacobsen SF, *et al*. Incidence and clinical presentation of pheochromocytoma and sympathetic paraganglioma: a population-based study. *J Clin Endocrinol Metab*. 2021;106(5):e2251-e2261.
4. Angelousi A, Kassi E, Zografos G, Kaltsas G. Metastatic pheochromocytoma and paraganglioma. *Eur J Clin Invest*. 2015;45(9):986-997.
5. Chang CA, Pattison DA, Tothill RW, *et al*. 68Ga-DOTATATE and 18F-FDG PET/CT in paraganglioma and pheochromocytoma: utility, patterns and heterogeneity. *Cancer Imaging*. 2016;16(1):22.
6. Sharma P, Dhull VS, Arora S, *et al*. Diagnostic accuracy of 68Ga-DOTANOC PET/CT imaging in pheochromocytoma. *Eur J Nucl Med Mol Imaging*. 2014;41(3):494-504.
7. Raffel DM, Jung YW, Koeppe RA, *et al*. First-in-Human studies of [18F] fluorohydroxyphenethylguanidines. *Circulation Cardiovascular Imaging*. 2018;11(12):e007965.
8. Raffel DM, Crawford TC, Jung YW, *et al*. Quantifying cardiac sympathetic denervation: first studies of 18F-fluorohydroxyphenethylguanidines in cardiomyopathy patients. *Eur J Nucl Med Mol Imaging*. 2022;49(2):619-631.
9. Wong KK, Else T, Viglianti BL, Brooks AF, Frey KA, Raffel DM. PET imaging of metastatic paraganglioma using novel 3-[18F] fluoro-para-hydroxyphenethylguanidine (3-[18F]pHPG) radiotracer. *Eur J Nucl Med Mol Imaging*. 2022;49(6):2098-2099.
10. Bombardieri E, Giammarile F, Aktolun C, *et al*. 131I/123I-metaiodobenzylguanidine (mIBG) scintigraphy: procedure guidelines for tumour imaging. *Eur J Nucl Med Mol Imaging*. 2010;37(12):2436-2446.
11. Jung YW, Jang KS, Gu G, *et al*. [18F]Fluoro-Hydroxyphenethylguanidines: efficient synthesis and comparison of two structural isomers as radiotracers of cardiac sympathetic innervation. *ACS Chem Neurosci*. 2017;8(7):1530-1542.
12. Jung YW, Gu G, Raffel DM. Improved synthesis of 4-[18F] fluoro-m-hydroxyphenethylguanidine using an iodonium ylide precursor. *J Labelled Comp Radiopharm*. 2019;62(12):835-842.
13. Pinsard M, Mouchet N, Dion L, *et al*. Anatomic and functional mapping of human uterine innervation. *Fertil Steril*. 2022;117(6):1279-1288.
14. Pandit-Taskar N, Zanzonico P, Staton KD, *et al*. Biodistribution and dosimetry of 18F-meta-fluorobenzylguanidine: a first-in-human PET/CT imaging study of patients with neuroendocrine malignancies. *J Nucl Med*. 2018;59(1):147-153.
15. Wang P, Li T, Cui Y, *et al*. 18F-MFBG PET/CT is an effective alternative of 68Ga-DOTATATE PET/CT in the evaluation of metastatic pheochromocytoma and paraganglioma. *Clin Nucl Med*. 2023;48(1):43-48.
16. Han S, Suh CH, Woo S, Kim YJ, Lee JJ. Performance of 68Ga-DOTA-conjugated somatostatin receptor-targeting peptide PET in detection of pheochromocytoma and paraganglioma: a systematic review and metaanalysis. *J Nucl Med*. 2019;60(3):369-376.
17. Kong G, Schenberg T, Yates CJ, *et al*. The role of 68Ga-DOTA-octreotate PET/CT in follow-up of SDH-associated pheochromocytoma and paraganglioma. *J Clin Endocrinol Metab*. 2019;104(11):5091-5099.
18. Şimşek DH, Şanlı Y, Kuyumcu S, Başaran B, Mudun A. 68Ga-DOTATATE PET-CT imaging in carotid body paragangliomas. *Ann Nucl Med*. 2018;32(4):297-301.